Analysis of Hairpin Ribozyme Base Mutations in Loops 2 and 4 and Their Effects on *cis*-Cleavage *in Vitro*†

Andrew Siwkowski, Richard Shippy, and Arnold Hampel*

Department of Biological Sciences, Northern Illinois University, DeKalb, Illinois 60115

Received November 20, 1996; Revised Manuscript Received January 24, 1997⊗

ABSTRACT: In order to determine base requirements in loops 2 and 4 of the hairpin ribozyme, a comprehensive mutational analysis of the wild type sequence was done. Each base position in these two loops was mutated to contain each of the three non-wild type bases, and the effects of these mutations were analyzed using *cis*-cleavage assays. The method of data analysis allowed for the determination of self−cleavage rates as well as the fraction of transcripts produced which were uncleavable. Three positions in loop 2 (A_{22}, A_{23}, and C_{25}) and one position in loop 4 (A_{38}) resulted in no detectable self-cleavage when mutated to any of the non-wild type bases. The remainder of the base positions showed varying degrees of tolerance to base mutations with respect to their support of *cis*-cleavage. Evidence was obtained for the presence of a non-Watson−Crick base pair between A_{26} and G_{36} in the catalytic conformation of the hairpin ribozyme. On the basis of these results, a two-dimensional model for the hairpin ribozyme is presented.

The hairpin ribozyme belongs to a small group of RNA enzymes capable of cleaving a phosphodiester bond at a specific site in RNA, leaving products containing 2′,3′-cyclic phosphate and 5′ OH termini at the site of cleavage [reviewed in Long and Uhlenbeck (1993)]. Since the discovery that the negative strand of the satellite RNA of tobacco ringspot virus [(−)sTRSV][1] was able to undergo self-cleavage (Gerlach et al., 1986; Buzayan et al., 1986), the minimum sequence required for catalysis, the secondary structure of the sequence and the ability for the motif to be adapted for trans cleavage of heterologous RNA was determined resulting in naming of the sequence as the hairpin ribozyme (Hampel & Tritz, 1989; Hampel et al., 1990; Anderson et al., 1994). A detailed kinetic analysis for both the ligation and cleavage activities of this ribozyme has been carried out (Hegg & Fedor, 1995). Recently the hairpin ribozyme has proven useful for gene therapy in human systems and is currently entering human clinical trials as an AIDS therapeutic (Welch et al., 1996).

Two other naturally occurring hairpin ribozymes have been identified and their cleavage activities characterized to date (DeYoung et al., 1995). These three ribozymes are derived from the minus strands of satellite RNAs associated with tobacco ringspot virus (−)sTRSV, chicory yellow mottle virus (−)sCYMV1, and arabis mosaic virus (−)sArMV. All three ribozymes conform to the hairpin ribozyme two-dimensional structure which has been determined for the (−)sTRSV ribozyme (Hampel et al., 1990; Anderson et al., 1994) (Figure 1). This model has 17 Watson−Crick base pairs found in two helical regions (helices 1 and 2) between the ribozyme and substrate and two helical regions (helices 3 and 4) within the ribozyme. Five single-stranded loop regions are located between the helices. The high level of phylogenetic base conservation within loops 2 and 4 among these three ribozymes strongly suggests either base requirements or base preferences in this region for supporting

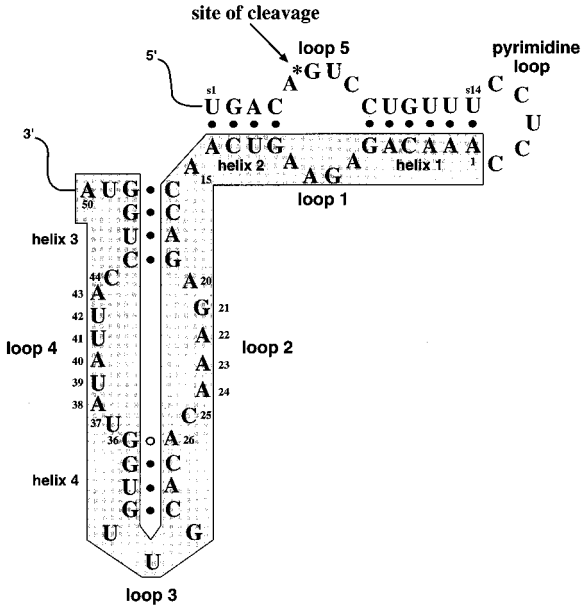

FIGURE 1: Hairpin ribozyme−substrate autocatalytic RNA two-dimensional model. The model contains the standard four helices (helices 1−4) and five loops (loops 1−5) named and numbered as originally described for the hairpin ribozyme (Hampel et al., 1990; Anderson et al., 1994). Base-specific mutagenesis was carried out in loop 2 (A_{20}−A_{26}) and loop 4 (G_{36}−C_{44}). The effect of base changes on catalysis was determined based on the level of self-cleavage supported by transcripts containing the mutations. The autocatalytic RNA consisted of substrate coding sequence (s1−s14), pyrimidine loop (CCUCC), and ribozyme coding sequence (1−50), respectively. Shown is the non-Watson−Crick A_{26}:G_{36} base pair identified in this study. The model is modified from the originally proposed L-shaped configuration (Hampel et al., 1989; Altschuler et al., 1992).

† Supported by NIH Grant R01AI29870 to A.H.

* To whom correspondence should be addressed.

⊗ Abstract published in *Advance ACS Abstracts,* March 15, 1997.

[1] Abbreviations: (−)sTRSV, the negative strand of the satellite RNA of tobacco ringspot virus; (−)sCYMV1, the negative strand of the satellite RNA of chicory yellow mottle virus; (−)sArMV, the negative strand of the satellite RNA of arabis mosaic virus; DTT, dithiothreitol; PEG, polyethylene glycol; FS, full-length autocatalytic RNA transcript; 3′P, the 3′ cleavage product; 5′P, the 5′ cleavage product.

S0006-2960(96)02873-5 CCC: $14.00

Chart 1

Loop 4 Primer #1:

TAATACGACTCACTATAGGGATCCTTTTTTTTTTTTTGACAGTCCTGTTTCCTCCAAACAGAG

Loop 4 Primer #2:

G_{36}: GCCGAAGCTTGCAGTCCTGCAGGTCGACTACCAGGTAATATA**N**CACAACGTGTGTTTCTCTGG
U_{37}: GCCGAAGCTTGCAGTCCTGCAGGTCGACTACCAGGTAATAT**N**CCACAACGTGTGTTTCTCTGG
A_{38}: GCCGAAGCTTGCAGTCCTGCAGGTCGACTACCAGGTAATA**N**ACCACAACGTGTGTTTCTCTGG
U_{39}: GCCGAAGCTTGCAGTCCTGCAGGTCGACTACCAGGTAAT**N**TACCACAACGTGTGTTTCTCTGG
A_{40}: GCCGAAGCTTGCAGTCCTGCAGGTCGACTACCAGGTAA**N**ATACCACAACGTGTGTTTCTCTGG
U_{41}: GCCGAAGCTTGCAGTCCTGCAGGTCGACTACCAGGTA**N**TATACCACAACGTGTGTTTCTCTGG
U_{42}: GCCGAAGCTTGCAGTCCTGCAGGTCGACTACCAGGT**N**ATATACCACAACGTGTGTTTCTCTGG
A_{43}: GCCGAAGCTTGCAGTCCTGCAGGTCGACTACCAGG**N**AATATACCACAACGTGTGTTTCTCTGG
C_{44}: GCCGAAGCTTGCAGTCCTGCAGGTCGACTACCAG**N**TAATATACCACAACGTGTGTTTCTCTGG

catalysis. Only one base position in each loop 2 and loop 4 exhibits variation among the three naturally occurring hairpin ribozymes. These are A_{20} and C_{44} of the (−)sTRSV ribozyme.

While the helical regions in the (−)sTRSV hairpin ribozyme have been established using mutagenesis (Hampel et al., 1990; Anderson et al., 1994) and further supported by *in vitro* selection procedures (Berzal-Herranz et al., 1993), the role of bases in the loops is less well understood. The ribozyme−substrate complex likely folds into a paperclip-like 3-dimensional structure using A_{15} as a hinge (Feldstein & Bruening 1993; Komatsu et al., 1994; Anderson et al., 1994), allowing loops 4 and 5 to come in close proximity to each other. Mutational analysis can provide information about specific base requirements for catalytic activity. Results from cleavage/ligation using *in vitro* selection techniques indicated that bases G_{21}, A_{22}, A_{23}, A_{24}, and C_{25} of loop 2 (Berzal-Herranz et al., 1993) as well as A_{38}, U_{41}, U_{42}, and C_{44} of loop 4 are required for cleavage−ligation (Berzal-Herranz et al., 1992).

Here we report the results of a comprehensive mutational analysis of all bases found in loops 2 and 4 of the hairpin ribozyme. The method was a direct point mutation approach wherein each base in loops 2 and 4 was changed individually to each of the three non-wild type nucleotides, and the rate of cleavage determined for each by measuring the unimolecular rate constant. Base requirements for *cis*-cleavage gave a range of base specific biases. These biases varied from the ability of the position to accommodate all four bases (A, C, G, U) without significant loss of activity to those capable of accommodating no other base besides the wild type sequence. The only bases required, within the limits of detection, were A_{22}, A_{23} and C_{25} in loop 2 and A_{38} in loop 4. Mutational analysis identified a non-canonical A_{26}:G_{36} base pair in helix 4 to give a hairpin secondary structure consisting of a total of 18 bp. Based on these and previously published results, a two-dimensional model for the hairpin ribozyme is presented (Figure 1).

MATERIALS AND METHODS

Hairpin Ribozyme cis-Cleaving Construct. The *cis*-cleaving hairpin ribozyme−substrate autocatalytic RNA of Figure 1 was used for these studies (Altschuler et al., 1992). Shown is the model with the standard four helices (helices 1−4) and five loops (loops 1−5) named and oriented as originally described for the hairpin ribozyme (Hampel et al., 1990; Anderson et al., 1994). Base-specific mutagenesis was carried out in loop 2 (A_{20}−A_{26}) and loop 4 (G_{36}−C_{44}).

Loop 4 Mutagenesis. Mutations for every nucleotide were inserted in each of the nine positions in loop 4 (G_{36}−C_{44}) (Figure 1). Mutation primers (primer #2) were randomized individually at each of these nine positions in loop 4. Randomized positions in loop 4 primer #2 for G_{36}, A_{38}, U_{41}, and U_{42} were created during DNA synthesis by drawing from an equimolar mixture of adenosine, cytidine, guanosine, and uridine phosphoramidites. The randomized positions in loop 4 primer #2 for the remainder of base mutations were made by drawing from an equimolar phosphoramidite mix containing only the non-wild type bases. This use of only three bases in the phosphoramidite mix increased the probability of obtaining clones representing all three non-wild type variants with fewer sequencing reactions. Chart 1 lists the PCR primers used in generating coding fragments for loop 4 mutants.

Each primer #2 is designated by the nucleotide numbered in Figure 1. The position in the DNA corresponding to this position is designated by **N**. This is the position which was randomized. PCR of the DNA was done with plasmid pHC (Altschuler et al., 1992) which contained the DNA sequence coding for the autocatalytic RNA. PCR was carried out by mixing together pHC DNA (2 μg), primer #1 and mutation primer #2 under standard PCR conditions.

The PCR products were the DNA for the autocatalytic RNA with the various mutations. This was digested with *Bam*HI/*Hin*dIII and cloned into pBluescript II K/S (Stratagene). The resulting constructs were sequenced to determine the base identity at the randomized position and to verify that no other mutations had occurred within the region to be transcribed. In this way all 27 possible single-point variants in loop 4 (nine bases with three variants at each position) were isolated. The resulting plasmids allowed for production of the autocatalytic RNA shown in Figure 1 by T7 transcription using a promoter upstream of the ribozyme coding region. The wild type sequence construct was isolated from the A_{38} clones, whose loop 2 primer #2 base randomization included the wild type base in the phosphoramidite mix. The wild type sequence construct was termed pGMC (Figure 2).

Loop 2 Mutagenesis. For studies on loop 2 mutants, it was desirable to utilize the *Dra*III site, located in helix 4/loop 3 of the hairpin ribozyme, as a cloning site for mutation-containing inserts. Before this could be done a second *Dra*III site had to be removed from the f1 origin of the plasmid pGMC. The plasmid pGMC was partially digested with *Dra*III. The full-size linearized plasmid was gel-isolated, and the 3′ overhangs were removed by treatment with T4

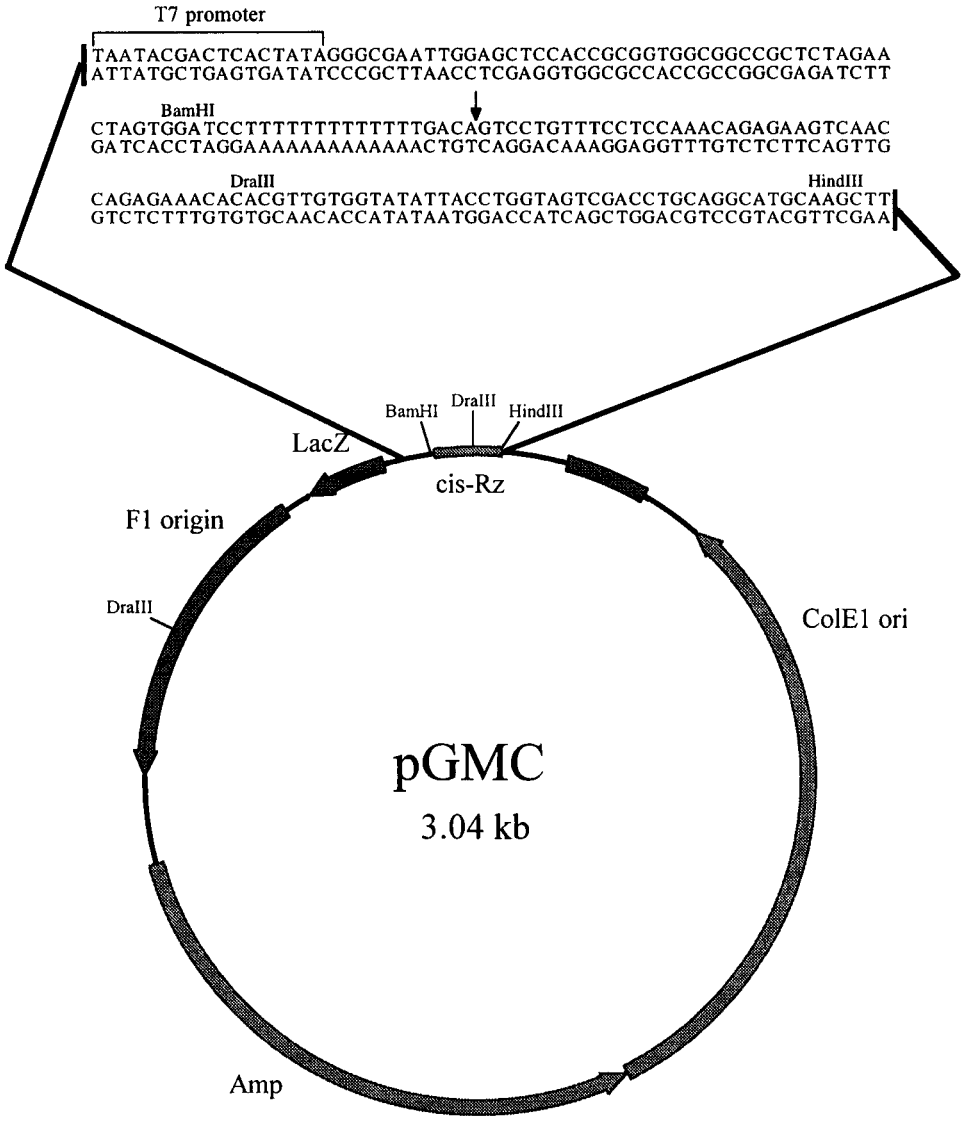

FIGURE 2: Plasmid pGMC coding for autocatalytic RNA. This plasmid contains the autocatalytic RNA of Figure 1 cloned into *Bam*H1/*Hin*dIII of pBluescript II K/S. This plasmid was used for all loop 4 mutagenesis. For loop 2 mutagenesis the *Dra*III originally located in the f1 origin was removed.

DNA polymerase. The DNA was re-ligated with T4 DNA ligase, cloned, and screened for loss of the *Dra*III site originally located in the plasmid's f1 origin and retention of the *Dra*III located within the ribozyme. The resulting plasmid was named pL2GMC. The *Dra*III site in the ribozyme region of pL2GMC was used as an insertion site for loop 2 mutants. Again, each of the seven positions in loop 2, $A_{20}-A_{26}$, were mutagenized to each of the non-wild type bases to give a complete mutant plasmid panel.

Double-stranded DNA fragments were synthesized using PCR by extension of primer dimers, each containing a randomized base position corresponding to the seven base positions found in loop 2 for the hairpin ribozyme. Base randomizations allowed for the incorporation of all but the wild type base identity during DNA synthesis of loop 2 primer #2. Primers used for the generation of loop 2 mutant coding fragments are shown in Chart 2.

The DNA fragments were digested with *Bam*HI and *Dra*III and cloned into pL2GMC. All plasmids were sequenced to determine base composition at the randomized position as well as to verify the remaining coding sequence of the transcript to be produced. Representatives of each mutation for all seven base positions were generated in this way, yielding a panel of 21 mutant clones.

Transcription of Wild Type and Mutant Ribozymes. Plasmid DNA from each mutant, as well as from the construct containing the wild type sequence, was digested with *Hin*dIII. The digest products were phenol/chloroform extracted, ethanol precipitated, washed, and vacuum dried. The DNA pellets were resuspended in 25 μL of H_2O and prewarmed at 37 °C for 5 min and transcribed using the T7 RNA polymerase system (Milligan et al., 1987). The transcription reactions were initiated with the addition of 50 μL of transcription mix which was also prewarmed at 37 °C. The composition of the final reactions was as follows: 5 μg of plasmid DNA, 40 mM Tris, pH 8.0, 6 mM $MgCl_2$, 5 mM DTT, 1 mM spermidine, 4% PEG-3000, 0.1% Triton X-100, 1 mM NTP, 20 μCi of [α-^{32}P]CTP, 20 units of RNasin (Promega), and 40 units of T7 RNA polymerase (Ambion). To initially screen for appropriate time points to be taken, reactions were incubated at 37 °C for a total of 20, 40, or 60 min. The resulting data were used to determine appropriate incubation times for the determination of catalytic parameters of each mutant. To generate kinetic data, reactions were incubated at 37 °C for a total of 15, 30, or 60 min, as determined appropriate from the initial transcription results, during which five time points were taken to define the curve. Reactions were terminated by additon of

Chart 2

Loop 2 Primer #1:

GCTCTAGAACTAGTGGATCCTTTTTTTTTTTTTGACAGTCCTGTTTCCTCCAAACAGAG
AAGTCAACCAG

Loop 2 Primer #2:

A_{20}: GTAATATACCACAACGTGTGTTTCNCTGGTTGACTTCTCTGTTTG
G_{21}: GTAATATACCACAACGTGTGTTTNTCTGGTTGACTTCTCTGTTTG
A_{22}: GTAATATACCACAACGTGTGTTNCTCTGGTTGACTTCTCTGTTTG
A_{23}: GTAATATACCACAACGTGTGTNTCTCTGGTTGACTTCTCTGTTTG
A_{24}: GTAATATACCACAACGTGTGNTTCTCTGGTTGACTTCTCTGTTTG
C_{25}: GTAATATACCACAACGTGTNTTTCTCTGGTTGACTTCTCTGTTTG
A_{26}: GTAATATACCACAACGTGNGTTTCTCTGGTTGACTTCTCTGTTTG

an equal amount of formamide dye, heated to 95 °C for 5 min, snap-cooled on ice, and loaded on 10% PAGE, 7 M urea gels. RNA was detected using autoradiography and bands corresponding to uncleaved RNA (FS), 3′ cleavage product (3′P), and background control (B) were excised from the gels and radioactivity determined by liquid scintillation counting. The cleavage percentage was calculated and converted to uncleaved fraction.

The resulting data from each time point were used in nonlinear regression analysis to fit to eq 1:

$$\text{uncleaved fraction} = [(1 - b)(1 - e^{-kt})/kt] + b \quad (1)$$

The term k is the unimolecular rate constant for self-cleavage (min^{-1}), t is reaction time (min), and b is the fraction of full-size RNA produced which is uncleavable [equation modified from Long and Uhlenbeck (1994)]. Both k and b were calculated from the data using a curve fitting program TableCurve 2D version 3 for WIN32 from Jandel Scientific. Most curve fits had statistical r^2 values of 0.99, and all had values greater than or equal to 0.95.

trans-Cleavage and Ligation Assays. The plasmids containing the $A_{38}C$ mutation and the $C_{44}G$ mutations were transcribed using [α-^{32}P]CTP as above. The bands corresponding to full-size RNA with the $A_{38}C$ mutation and those corresponding to the 3′ product of RNA containing the $C_{44}G$ mutation, were excised from the gel and ground in 500 μL of 0.5 M ammonium acetate, 2 mM Na_2EDTA, and 0.5 mg/mL of SDS. The RNA was shaken at room temperature for 1 h, centrifuged to pellet the gel particles, ethanol precipitated, and redissolved in water. These two RNAs were used to measure possible *trans*-cleavage and ligation events as follows.

To measure possible *trans*-cleavage, the plasmid pGMC (Figure 2) was transcribed to give the wild type autocatalytic RNA transcript. Transcription was carried out as above without any ^{32}P nucleotide label (unlabeled reaction) but in the presence of 50 nM ^{32}P internally labeled $A_{38}C$ full-length transcript. A control transcription reaction was done simultaneously with 20 μCi of [α-^{32}P]CTP (labeled) in the absence of $A_{38}C$ full-length transcript. Time points were removed at 0, 12, 24, 36, 48, and 60 min.

To measure possible ligation of the cleaved RNA, the plasmid pGMC was transcribed as above, but without added [α-^{32}P]CTP (unlabeled) and in the presence of 25 nM ^{32}P internally labeled $C_{44}G$ 3′ product. A control transcription using 20 μCi of [α-^{32}P]CTP was run simultaneously. Time points were removed at 0, 12, 24, 36, 48, and 60 min.

RESULTS AND DISCUSSION

In order to determine base requirements in loops 2 and 4, an extensive mutational analysis was undertaken. The constructs employed used the *cis*-cleaving hairpin ribozyme consisting of four helices (helices 1−4) interspersed with five single-stranded loops (Figure 1). Base-specific mutagenesis was carried out in loop 2 (A_{20}−A_{26}) and loop 4 (G_{36}−C_{44}). Comparison of mutant self-cleavage kinetic rates with those of the wild type sequence was done for all mutations to all bases in loops 2 and 4.

Detection of trans-Cleavage during the Autocatalytic Reaction. Before the cleavage observed could be attributed to *cis*-cleavage, the possibility of *trans*-cleavage had to be ruled out, since, if present, it would have the effect of erroneously inflating the *cis*-cleaving unimolecular self-cleavage rate constant (k). In order to test whether *trans*-cleavage was occurring, a mutant which is later shown to support no detectable self-cleavage ($A_{38}C$) was transcribed and the full-size RNA was isolated. While this mutant contained a base change in loop 4, it retained the wild type substrate region, and could therefore serve as a substrate in a *trans*-cleavage event if that were indeed occurring. The RNA was then renatured and added to a nonradioactive transcription reaction which produced wild type sequence *cis*-cleaving RNA. This amount of added RNA was approximately 1/5 that of wild type transcript at the completion of the transcription reaction. That is, there was a 5× excess of wild type transcript to drive the *trans*-reaction if it were to occur. There was no visually detectable cleavage of the $A_{38}C$ mutant RNA throughout the time of reaction in the presence of an excess of wild type sequence RNA, which was undergoing self-cleavage, indicating *trans*-cleavage was not occurring (Figure 3A, left panel). The $A_{38}C$ mutant RNA was stable under the transcription reaction conditions throughout the 60 min reaction time.

A parallel transcription reaction was used to verify the production of wild type sequence transcripts in the nonradioactive transcription reaction (Figure 3A, right panel). This second reaction was identical to the first, except that it lacked the $A_{38}C$ RNA and included [α-^{32}P]CTP. The results also verified the rate of transcript production was approximately linear with respect to time throughout the reaction.

In order to verify that the inability of self-cleavage to go to completion was not caused by the establishment of an equilibrium between cleavage and ligation reactions, an experiment was performed utilizing the 3′ product from self-cleavage of the $C_{44}G$ mutant. This particular mutant had a

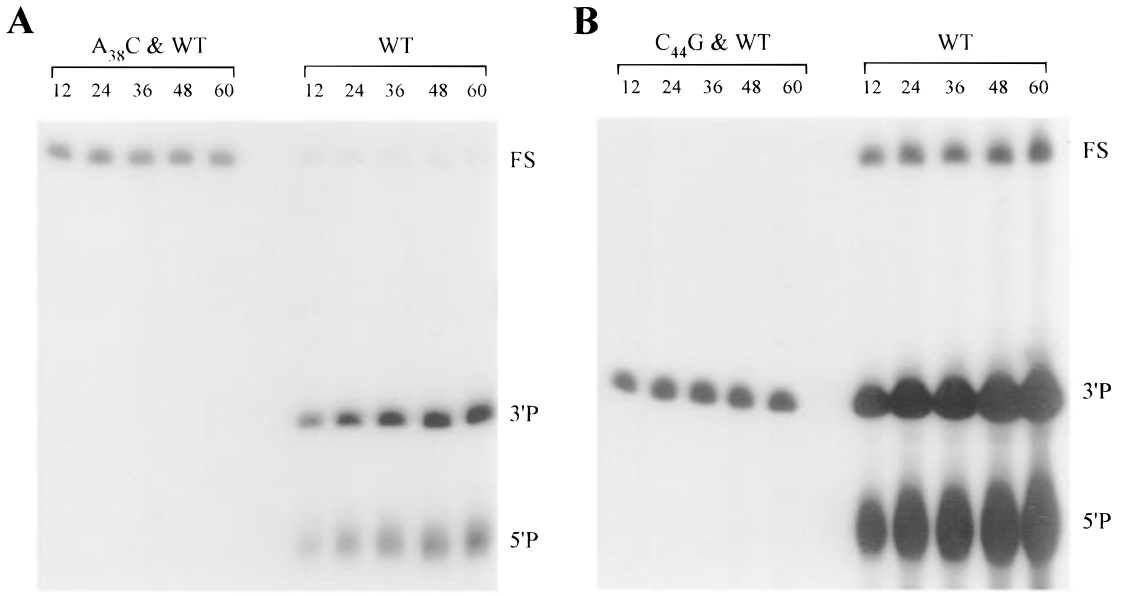

FIGURE 3: Transcription time courses for measurement of *trans*-cleavage and ligation activities of autocatalytic RNA. (A) Left panel ($A_{38}C$ and WT). Transcription of wild type sequence autocatalytic RNA (unlabeled) with added internally labeled ^{32}P labeled $A_{38}C$ RNA. The inability to detect product formation from $A_{38}C$ RNA indicates that *trans*-cleavage activity was not detectable. Right panel (WT). Transcription of wild type sequence autocatalytic RNA using [α-^{32}P]CTP (labeled) and without added $A_{38}C$ RNA. (B) Left panel ($C_{44}G$ and WT). Transcription of wild type sequence autocatalytic RNA (unlabeled) in the presence of added ^{32}P internally labeled $C_{44}G$ RNA 3′ product. The absence of reformation of $C_{44}G$ full-size RNA in the left panel indicates that the extent of ligation is not detectable. Right panel (WT). Transcription of wild type sequence autocatalytic RNA with [α-^{32}P]CTP (labeled) and without added $C_{44}G$ 3′ product. For both A and B, above each lane is the time (min) at which the reaction was terminated. FS, full-size transcript; (3′P) the 3′ cleavage product; and (5′P) the 5′ cleavage product.

unimolecular self-cleavage rate constant (k) of 0.13/min and produced an uncleavable fraction (b) of 0.74 (see below). Use of this mutant allowed for the recovery of sufficient 3′ product to be tested for its ligation capability. As was done in the *trans*-cleavage experiment described above, parallel transcription reactions were run. In the first reaction, ^{32}P-labeled $C_{44}G$ 3′ product was incubated in a nonradioactive wild type transcription reaction. The 5′ product from wild type *cis*-cleavage was identical to that originally produced by $C_{44}G$ during its self-cleavage and could therefore serve the same role in $C_{44}G$ ligation (if that were to occur) as 5′ product generated by $C_{44}G$ self-cleavage. Generation of the 5′ product during the transcription of wild type sequence ensures that the condition of the 2′,3′-cyclic phosphate created at the cleavage site during wild type self-cleavage was identical to that present in the original $C_{44}G$ transcription reaction. Ligation activity would be evidenced by the appearance of a band comigrating with the full-size wild type RNA. The amount of added internally labeled RNA was 1/17 the amount of final wild type transcript. Thus there was a 17× excess of unlabeled wild type transcript to drive the ligation reaction if it were to occur. Even after a total incubation time of 60 min, no ligation product was observed (Figure 3B, left panel). Radioactivity quantitation and analysis confirmed that ligation activity was less than 1%. The uncleavable fraction, therefore, does not represent ligation activity. As noted in the previous experiment, the RNA was stable throughout the reaction and the rate of transcript production was linear with respect to time (Figure 3B, right panel).

There was an apparent heterogeneity in the length of 5′ products in each reaction. This phenomenon had previously been observed in studies involving *cis*-cleaving ribozyme cassettes utilizing hammerhead ribozymes, hepatitis D ribozymes, and hairpin ribozymes (Chowrira et al., 1994). Transcripts larger than coded for by the DNA template were explained as the addition of extra guanosines incorporated on the 5′ end of the transcript by T7 RNA polymerase.

Mutations at A_{22}, A_{23}, and C_{25} in Loop 2 and A_{38} in Loop 4 Gave Undetectable Activity. Autocatalytic cleavage of hairpin catalytic RNA during the 60 min transcription reactions of the mutant and wild type clones showed no detectable cleavage for all mutations to A_{22}, A_{23}, or C_{25} of loop 2 as well as A_{38} of loop 4 (Figure 4). The lower limit for visually detectable self-cleavage of loop 2 mutants was 4.3% ± 1.4%, and that of loop 4 mutants was 2.4% ± 1.5%. Assuming an uncleavable fraction of 0.03, corresponding to that later found for the wild type sequence, minimum self-cleavage rates of 0.0016/min for loop 2 and 0.0009/min for loop 4 would be needed to produce visually detectable cleavage products. Cleavage of mutants at A_{22}, A_{23}, and C_{25} of loop 2 and at A_{38} of loop 4 are below these limits of detection.

Determination of Cleavage Rates and Inactive Conformers. The following equation (eq 2)

$$\text{fraction uncleaved} = (1 - e^{-kt})/kt \qquad (2)$$

had previously been used to demonstrate the effects of hammerhead ribozyme base mutations on catalysis (Long & Uhlenbeck 1994). It was necessary, however, in our study to modify this equation to include the uncleavable fraction (b) which occurred for the various mutations.

The modification took the general form

$$\text{fraction uncleaved} = [(1 - b)a] + b \qquad (3)$$

where a represents the right half of eq 2. In its final form the equation used is as shown in eq 1. The presence of an uncleavable fraction during the reaction was evidenced by a b value greater than zero. While this particular reaction model allows for the segregation of effects from k and the uncleavable subpopulation when self-cleavage is observed,

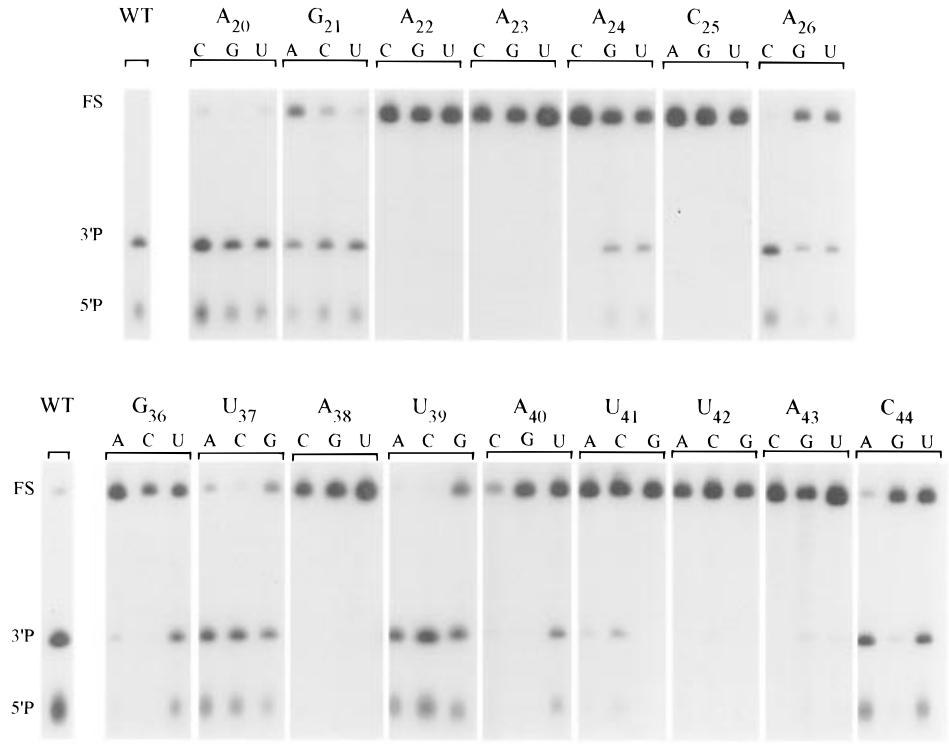

FIGURE 4: Cleavage of hairpin autocatalytic RNA. Linearized plasmids were transcribed for 60 min, during which the RNA transcript was autocatalytically cleaved. Reaction products were separated on 10% PAGE, 7 M urea gels. Shown on each panel is the identity of the wild type base which was mutated to each of the remaining three bases. WT, wild type sequence; FS, full-length autocatalytic RNA transcript; 3′P, the 3′ cleavage product; 5′P, the 5′ cleavage product.

it is unable to differentiate between a large uncleavable population and a very low *k* value. Therefore, the determination of extremely low *k* values from the data becomes problematic. The reporting of such values is therefore omitted from this report. This leaves open the possibility that point mutations which prevent self-cleavage produce uncleavable fractions approaching 1.0 rather than having *k* values approaching zero.

Determination of Rate of Cleavage and Uncleavable Fractions for All Mutations to All Bases in Loops 2 and 4. Mutations to all positions in loops 2 and 4 were made, the constructs transcribed, aliquots were removed at various times, full-size RNA and products from autocatalytic cleavage were separated by gel electrophoresis, products and reactants quantitated, the fraction that was uncleaved was analyzed by eq 1, and *k* and *b* values were calculated. This was done for all mutations to the seven positions $A_{20}-A_{26}$ of loop 2 and for all mutations to the nine postions $G_{36}-C_{44}$ in loop 4 (Figure 5 and Table 1). As a way of more meaningful comparison, *k* values for each mutant were also calculated relative to that of the wild type sequence to give the ratio of k_{wt}/k_{mut} (Table 1).

Several bases in loops 2 and 4 of the hairpin ribozyme appear not only to serve the role of contributing to essential interactions for catalysis but also to prevent the formation of noncatalytic conformations. It therefore appears that what the bases prevent is as important as what they allow. The formation of an uncleavable fraction, with a range of *b* values depending on the mutation, was evident for many of the mutations (Table 1). This was likely due to alternate inactive conformations being trapped in kinetically stable conformations (Herschlag, 1995). Previous work using a *cis*-cleaving hairpin ribozyme determined that the self-cleavage reaction often did not go to completion. As little as 60% of hairpin ribozyme-based *cis*-cleaving RNA produced during transcription underwent self-cleavage (Altschuler et al., 1992). It was also noted that eq 2 was unable to fit hammerhead ribozyme self-cleavage data, presumably due to the formation of alternate conformers caused by flanking sequences (Chowrira et al., 1994).

A base by base description of the results, found in Figures 4 and 5 and Table 1, and a discussion of their significance follows.

A_{20}

A_{20} could be changed to any of the other three bases without significant loss of activity. In fact, activity increased with $A_{20}C$ and $A_{20}U$ mutations. This result was consistent with previously reported results that an adenine was not required in this position for cleavage (Anderson et al., 1994; Berzal-Herranz et al., 1993). This is the only base whose identity varies among all three of the naturally occurring hairpin ribozymes found to date (DeYoung et al., 1995). The summation of these observations is that the functional groups of this base are not involved in any critical interactions either within the ribozyme−substrate complex or with the complex's external environment.

Some type of base may be required since it has been reported that an abasic construct at A_{20} supports only 1.4% of the catalytic efficiency (k_{cat}/K_M) of the base-containing ribozyme (Schmidt et al., 1996). This large decrease in efficiency was attributed to the involvement of A_{20} in an important stacking interaction. However, it is clear from our results that such a proposed stacking interaction is not base specific.

The decrease in activity of $A_{20}G$ may be explained by the ability of the G_{20} mutant to extend helix 3 by forming a canonical Watson−Crick base pair with C_{44}. If this is the

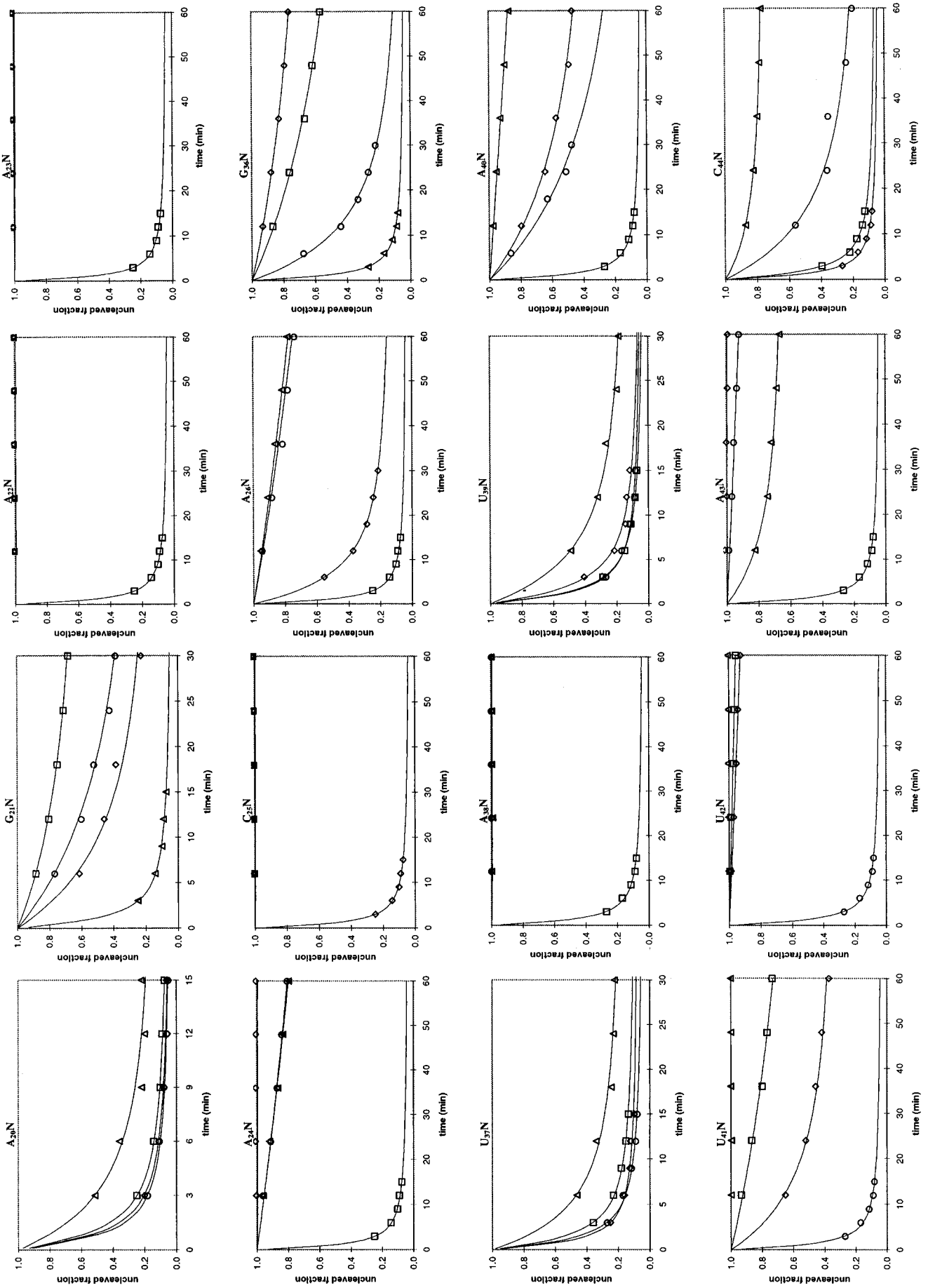

FIGURE 5: Self-cleavage kinetics of mutants. The uncleaved fraction as a function of time was analyzed by eq 3 to determine the unimolecular rate constant (k) and the uncleavable fraction (b). Each graph is the result of mutation to each of the remaining three bases for that position in the ribozyme sequence. □ = A, △ = G, ◇ = C, and ○ = U.

Table 1: Kinetic Analysis of Loop 2 Loop 4 Mutants[a]

nat base	mutation	k (min^{-1})	k_{wt}/k_{mut}	uncleaved fr (b)	r^2
		Loop 2 Mutants			
wt	none	1.46	–	0.03	>0.99
A_{20}	C	1.8	0.8	0.02	0.99
	G	0.59	2.5	0.09	0.96
	U	2.0	0.7	0.02	>0.99
G_{21}	A	0.10	15	0.54	>0.99
	C	0.19	7.7	0.09	0.97
	U	0.11	13	0.14	>0.99
A_{22}	C*	<0.0016	>900	–	–
	G*	<0.0016	>900	–	–
	U*	<0.0016	>900	–	–
A_{23}	C*	<0.0016	>900	–	–
	G*	<0.0016	>900	–	–
	U*	<0.0016	>900	–	–
A_{24}	C*	<0.0016	>900	–	–
	G	0.008	180	0.00	0.99
	U	0.010	150	0.24	>0.99
C_{25}	A*	<0.0016	>900	–	–
	G*	<0.0016	>900	–	–
	U*	<0.0016	>900	–	–
A_{26}	C	0.26	5.6	0.10	>0.99
	G	0.008	180	0.00	>0.99
	U	0.012	120	0.11	0.99
		Loop 4 Mutants			
wt	none	1.30	–	0.03	0.99
G_{36}	A	0.035	37	0.26	>0.99
	C	0.028	46	0.54	>0.99
	U	0.16	8.1	0.00	0.99
U_{37}	A	1.0	1.3	0.08	>0.99
	C	1.7	0.8	0.07	0.99
	G	0.40	3.3	0.14	0.98
A_{38}	C*	<0.0009	>1400	–	–
	G*	<0.0009	>1400	–	–
	U*	<0.0009	>1400	–	–
U_{39}	A	1.2	1.1	0.01	>0.99
	C	0.80	1.6	0.03	0.99
	G	0.32	4.1	0.09	0.99
A_{40}	C	0.060	22	0.27	0.99
	G	0.004	330	0.00	0.99
	U	0.059	22	0.00	0.99
U_{41}	A	0.023	57	0.42	0.99
	C	0.12	11	0.29	0.99
	G*	<0.0009	>1400	–	–
U_{42}	A	0.002	650	0.02	0.96
	C	0.003	430	0.00	0.99
	G*	<0.0009	>1400	–	–
A_{43}	C*	<0.0009	>1400	–	–
	G	0.11	12	0.62	0.99
	U	0.003	430	0.01	0.99
C_{44}	A	0.85	1.5	0.05	>0.99
	G	0.13	10	0.74	>0.99
	U	0.13	10	0.10	0.95

[a] Asterisks are used to indicate reactions where no cleavage occurred above the limits of detection. The lower limits of detection for k were 0.0016/min for loop 2 mutants and 0.0009/min for loop 4 mutants. A dash is used where a value could not be calculated from the data obtained.

cause of the decrease, it does not appear to produce a significantly larger uncleavable fraction. It is likely that $A_{20}G$ competes with another group for transient interaction with C_{44}, resulting in a lower k for this particular mutation.

G_{21}

All base mutations at this position retain significant catalytic activity indicating that this base also does not have functional groups involved in critical interactions for the ribozyme−substrate complex and catalysis. The decrease in activity by all G_{21} mutants approximates one order of magnitude. A particularly large uncleavable fraction (0.54) existed in the $G_{21}A$ reaction. No definitive explanation could be given for this; however, it is possible that this may be an artifact of this particular construct wherein the resulting stretch of five adenosines could base pair with the region of 12 unpaired uridines located immediately upstream of the substrate region of the transcript. The uncleavable fraction would thus represent a subpopulation of transcripts in an alternate non-catalytic conformation.

These results are consistent with previously published work reporting that $G_{21}C$ supports 58% of the cleavage activity of the wild type sequence (Anderson et al., 1994). However both studies do not agree with a report that all three G_{21} mutants were strong down-mutations for cleavage (Berzal-Herranz et al., 1993). An abasic substitution at this position supported only 0.2% of the catalytic efficiency of the wild type sequence (Schmidt et al., 1996). Further, it was shown that substitution of G_{21} with inosine, O^6-methylguanosine, or N^7-deazaguanosine resulted in a retention of only 1.2%−1.7% of the catalytic efficiency of that for wild type.

A_{22}

No cleavage was obtained for any A_{22} mutant within the limits of detection. Prior to this study the effects of the $A_{22}C$ mutation had not been determined. These results, however, are consistent with a previous study showing $A_{22}G$ and $A_{22}U$ both decreased catalysis below detectable levels (Berzal-Herranz et al., 1993). Analyses of base functional groups revealed loss of the exocyclic amino group resulted in a 92% decrease in catalytic efficiency, and loss of the N^7 position by substitution of N^7-deazaadenine for A_{22} lowered cleavage efficiency by 99.8% (Grasby et al., 1995). Decrease in activity due to the loss of N^7 as an available bonding site may partially explain the importance of A_{22}, however it does not explain the absence of cleavage in mutants containing $A_{22}G$ since the N^7 position would be retained. Overall, all results support lack of cleavage from mutations to this base which strongly suggests that it serves a key role in the catalytic reaction or structure.

A_{23}

No detectable cleavage was obtained for any A_{23} mutant above the limit of detection ($k \geq 0.0016$), showing that this base is critical for the reaction. In agreement with our results, these mutations were shown not to support cleavage (Berzal-Herranz et al., 1993). Removal of the exocyclic amino group of A_{23} gave a 91.3% decrease in catalytic efficiency, and loss of the N^7 of the purine backbone caused a loss of 89.4% in catalytic efficiency (Grasby et al., 1995). The approximate 10-fold decrease in catalytic efficiency from both functional group substitutions of this base are consistent with each being involved in an interaction. The significant increase in the catalytic rate constant of ribozymes containing each individual functional group substitution with increasing Mg^{2+} (Grasby et al., 1995) suggests that both the exocyclic amino group and the N^7 position are either directly or indirectly interacting with Mg^{2+}. In any case, all studies agree that this position is critical for catalysis.

A_{24}

No detectable cleavage was observed with the $A_{24}C$ mutant, and large decreases in cleavage rate were found for the other two non-wild type base substitutions at this position.

This position had previously been thought to be required for efficient cleavage as the result of its being completely retained by *in vitro* selection, and furthermore, the $A_{24}U$ was catalytically inactive (Berzal-Herranz et al., 1993). Functional group studies have shown that the exocyclic amino group of A_{24} is important in catalysis and also indicated that N^7 of this base is not involved in any key interactions (Grasby et al., 1995).

The inability to detect self-cleavage in $A_{24}C$ may be the result of formation of a thermodynamically favored 6 bp helix 4 utilizing bases $A_{23}-A_{38}$ and $U_{32}-U_{37}$. The possibility therefore exists that, rather than there being no cleavage due to an extremely low rate constant (k), activity was prevented by the vast majority of molecules forming an inactive conformation and thus representing a large uncleavable fraction. In the complete absence of detectable cleavage, differentiation of these two possibilities is not achievable, however, the existence of such an alternate conformation was supported by the finding of a very high uncleavable fraction (0.24) present in the $A_{24}U$ reaction (Table 1) since a similar, but weaker, 6 bp helix 4 could form, utilizing a $U_{24}-G_{36}$ base pair.

C_{25}

No detectable cleavage was found with any of the mutant bases occupying this position. With the base pairing between A_{26} and G_{36} explained below, C_{25} becomes the last (3′) base in loop 2. It is positioned directly opposite U_{37} which is shown to sustain less than a 4-fold reduction in activity when mutated to any of the other three bases (see below). It therefore appears unlikely that C_{25} interacts with U_{37}.

These results are in agreement with *in vitro* selection for cleavage and ligation, wherein all 15 catalytically active sequences retrieved retained C_{25}, and one sequence containing $C_{25}G$ was shown to be inactive (Berzal-Herranz et al., 1993). Both results agree that this is a critical base for some phase of the catalytic reaction.

A_{26} and G_{36}

All A_{26} mutants exhibited cleavage; however, both $A_{26}U$ and $A_{26}G$ had rates $>20\times$ less than that of the $A_{26}C$ mutation. This was likely due to the ability of the $A_{26}C$ mutant to form a G:C Watson−Crick base pair with G_{36} and thus extend helix 4 to four base pairs.

Position G_{36} also shows activity with each of the three non-wild type bases albeit quite low for $G_{36}A$ and $G_{36}C$. The $G_{36}U$ mutant has the highest activity of the three variants in this position. This particular base substitution also has the potential of forming an A:U Watson−Crick base pair with A_{26} of loop 2 and consequently extending helix 4 to four-base pairs in length. This further supports a hairpin ribozyme two-dimensional model with a four base helix 4 containing a non-canonical A_{26}:G_{36} base pair in the catalytic conformation. The significance of the base−base interaction between A_{26} and G_{36} probably lies in the stabilization of helix 4 and/or its positioning of C_{25}.

While not noted by the authors, results in a previous report support these findings by showing a strong A:G or Watson−Crick covariation (14/15 clones) between A_{26} and G_{36} (Berzal-Herranz et al., 1993). Chemical modification also suggested the existence of an interaction between A_{26} and G_{36} in the ground state structure of the hairpin ribozyme (Butcher & Burke, 1994b).

The significantly high uncleavable fractions associated with $G_{36}A$ and $G_{36}C$ mutants, which would prevent base pairing between the bases occupying positions 26 and 36, may be the result of a shift in the predominant structure of the helix 4/loop 3 hairpin stem. In the wild type sequence, an alternate 4 bp helix 4 can form involving $C_{25}-A_{28}$:$U_{32}-G_{35}$. This structure may well compete with the one that supports catalysis for formation in the wild type sequence. The bias would be shifted, however, by the disruption of the base pair between positions 26 and 36. No significant increase in uncleavable fraction was seen with non-base pairing mutations at position 26 since these mutants would also greatly reduce the potential for the formation of the alternate helix.

The hairpin ribozyme two-dimensional model, therefore, likely contains a 4 bp helix 4 with a non-Watson−Crick A_{26}:G_{36} base pair as the fourth base pair in this helix (Figure 1). Such a model extends the 3 bp helix 4 previously shown to exist (Hampel et al., 1990; Anderson et al., 1994), and it fits all available data analyzing these two positions.

U_{37}

The U_{37} position can easily accommodate any of the four bases with less than 4-fold loss of activity. The $U_{37}A$ and $U_{37}C$ mutations had no loss of activity, while the $U_{37}G$ mutation had a $3.3\times$ reduction in rate. The $U_{37}G$ mutation also had the highest uncleavable fraction indicating that perhaps the $U_{37}G$ mutant may form a G:C base pair with C_{25} directly opposite, causing a reduction in activity. The high degree of variability exhibited at this position from single-point mutational analysis indicates that no essential contacts involving the bases in these positions are made within the molecule in its catalytically active conformation.

This position previously was shown to support cleavage when occupied by either an A or C (Berzal-Herranz et al., 1993). It has further been shown that abasic substitution at this position results in the loss of 89% of the catalytic efficiency of the wild type ribozyme (Schmidt et al., 1996). The activity decrease found from the abasic substitution may be due to the loss of a base stacking interaction which is at least partially maintained with the mutations used in this study.

A_{38}

A_{38} was the only position in loop 4 for which no detectable cleavage occurred for any of the three mutants. The lower limit of detection was a catalytic rate 0.07% that of the wild type. Therefore the adenine most likely has a functional group critical to the catalytic step or the formation of an active ribozyme−substrate conformation. This is supported by the observation that loss of the exocyclic amino group from A_{38} is accompanied by a 300-fold decrease in k_{cat} (Grasby et al., 1995). It is therefore likely that the exocyclic amino group in position A_{38} is involved in a key interaction in the active ribozyme−substrate complex.

Of the six different sequences obtained through *in vitro* selection for cleavage and ligation, A_{38} displayed 100% conservation (Berzal-Herranz et al., 1992). It has also been shown that $A_{38}G$ supported only 2% of the activity of the wild type sequence and $A_{38}U$ resulted in the loss of measurable levels of cleavage (Anderson et al., 1994). The substitution of A_{38} with an abasic residue resulted in the retention of only 0.1% of the catalytic efficiency of the wild

type sequence (Schmidt et al., 1996), and substitution at this position with base analogs purine and N^7-deazaadenine caused reductions of catalytic efficiency to 0.4% and 4.6%, respectively (Grasby et al., 1995). Thus this is an important base for the catalytic reaction.

U_{39}

The U_{39} position is variable. No more than approximately a 4-fold reduction in cleavage rate accompanied the incorporation of any of the mutant bases in this position, indicating that U_{39} itself is involved in no key interactions within the ribozyme or with its external environment.

This position had previously been shown to support high levels of catalysis for the mutations $U_{39}C$ or $U_{39}G$ (Anderson et al., 1994); however, the $U_{39}A$ mutation had not been previously characterized. The $U_{39}C$ mutation has been suggested to be a general up-mutation (Berzal-Herranz et al., 1993); however, we find that this mutation does not increase catalytic rate but rather gives an approximately 40% reduction. The deletion of the base moiety from this position has little effect on cleavage efficiency (Schmidt et al., 1996), indicating that base stacking is not even involved in this position.

A_{40}

When this position was occupied by either of the pyrimidine bases, a 22-fold decrease in catalytic rate was seen. The $A_{40}G$ mutant, however, resulted in a much more dramatic (330×) rate decrease. One possible explanation for the large loss of activity by the $A_{40}G$ mutant is the formation of an inactive conformation which competes with the formation of the catalytically active one. This particular mutant has the ability to form a stem between loops 2 and 4 utilizing $A_{23}-A_{26}$:$U_{39}-U_{42}$. The resulting helix would be composed of four Watson−Crick type base pairs. It would be expected that such an inactive alternate conformation would increase the uncleavable fraction (*b*); however, because of the extremely slow rate of cleavage, it was difficult to measure the uncleavable fraction. Overall, our results show a strong bias for the conservation of A_{40}.

The absence of a base moiety at this position resulted in a loss of 99.8% of catalytic efficiency (Schmidt et al., 1996), indicating the base plays an important role in the catalytic structure. Neither N^7 nor the exocyclic amino group of this base appears to be involved in important interactions, however (Grasby et al., 1996). Previous mutational analyses have shown that $A_{40}G$ and $A_{40}U$ supported 3% of the cleavage activity of the wild type sequence (Anderson et al., 1994), and $A_{40}C$ has been reported to support cleavage/ligation by the hairpin ribozyme (Berzal-Herranz et al., 1992).

U_{41}

Our results showed that $U_{41}A$ and $U_{41}C$ mutations resulted in decreases in cleavage rate of 57× and 11×, respectively while no cleavage could be detected with $U_{41}G$. Thus U_{41} greatly facilitates but is not required for cleavage. Previous work showed U_{41} to be required for cleavage−ligation of the hairpin ribozyme based on 100% conservation of its base identity after *in vitro* selection (Berzal-Herranz et al., 1992). However, it has also been reported that $U_{41}C$ supports 25% of the cleavage activity found with the wild type sequence (Anderson et al., 1994). The importance of a base occupying this position is evidenced by the finding that an abasic substitution at this position results in a 99.7% decrease in catalytic efficiency (Schmidt et al., 1996).

U_{42}

Mutations in this position resulted in nearly complete loss of activity, with $U_{42}G$ giving no detectable cleavage. This extends previous work showing the deletion of the base from this position resulted in a 99.3% decrease in catalytic efficiency (Schmidt et al., 1996). U_{42} was reported to be required for cleavage/ligation (Berzal-Herranz et al., 1992), and $U_{42}C$ supported only 3% of the catalytic activity of the wild type sequence (Anderson et al., 1994). Thus overall, this is a highly critical base for the catalytic event.

A_{43}

Previous work has shown that $A_{43}G$ supported cleavage−ligation (Berzal-Herranz et al., 1992), and cleavage levels supported by $A_{43}U$ were undetectable (Anderson et al., 1994). It was also shown that absence of a base moiety at this position resulted in a retention of only 0.3% of the catalytic efficiency of the wild type sequence (Schmidt et al., 1996). Loss of N^7 by substitution with N^7-deazaadenine caused a loss of 99.8% of catalytic efficiency, whereas loss of the exocyclic amino group of adenine by purine substitution resulted in retention of 47% of catalytic efficiency (Grasby et al., 1995). These findings suggested that N^7 of A_{43} is involved in a key interaction necessary for catalysis.

The findings reported here are in good agreement with previous determinations showing N^7 of the base at A_{43} to be important for catalysis. The mutation to $A_{43}U$ showed a 430-fold decrease, and cleavage was not detectable for $A_{43}C$. However, the $A_{43}G$ mutation had only a 12-fold reduction in catalytic rate. The $A_{43}G$ would retain N^7 of the purine backbone so it could remain available for required interactions.

C_{44}

C_{44} previously was reported to be required for cleavage and/or ligation by the hairpin ribozyme based on its absolute conservation within six different sequences recovered in an *in vitro* selection scheme (Berzal-Herranz et al., 1992). Later research determined that when an abasic residue was used at this position, the ribozyme retained 37% of its catalytic efficiency indicating that it was not required (Schmidt et al., 1996). The results reported here, where all mutations resulted in decreases in cleavage activity of 1 order of magnitude or less, are consistent with the latter findings. Thus this base is not required.

A possible explanation for the discrepancy lies in the different activity assays used. The results from the earlier selection study reflect requirements for both cleavage and subsequent ligation. Those of the latter, as well as this study, reflect requirements for cleavage only. It is therefore plausible that C_{44} was required for ligation but not for cleavage. Further work needs to be done before this can be more firmly stated. In any event, this is a highly variable position.

Variability in this position is further supported by phylogenetic comparison with the sCYMV1 hairpin ribozyme which has a uridine in this position and maintains high catalytic activity (DeYoung et al., 1995). It is noteworthy that $C_{44}U$, which is found in the sCYMV1-derived hairpin

ribozyme, resulted in a 10-fold decrease in catalytic rate compared to the wild type base in the sTRSV derivative. It appears likely that A_{20} and C_{44} co-vary among the three naturally occurring hairpin ribozyme variants so as not to form Watson−Crick base pairs between these two base positions.

In the study reported here, analysis of point mutations in this position showed significant activity was obtained from variants in this position. The C_{44}A mutant retained cleavage rates approaching those of the wild type sequence, while C_{44}G and C_{44}U supported cleavage 1 order of magnitude less than the wild type sequence, similar to decreases accompanying the aforementioned abasic substitution. These results suggest that C_{44} is involved in one interaction.

The unusually large uncleavable fraction (0.74) produced with the C_{44}G mutation may reflect the formation of an extended helix 3 encompassing bases $C_{16}-A_{23}$ and $U_{41}-G_{48}$. The resulting helix would include an internal A−G tandem pairing (A_{20}:C_{44}G and G_{21}:A_{43}). Tandem A−G pairs have similar energies of formation as the more widely studied tandem G−A pairs, indicating that they would have a high likelihood of forming in this structural environment (SantaLucia et al., 1990).

Model for Interactions. Previous models were suggested for additional interactions of bases between loops 2 and 4. It has been proposed that $G_{21}-A_{23}$ and $U_{39}-A_{43}$ are involved in the formation of a structure similar to one found in loop E of 5S rRNA on the basis of sequence similarities and UV sensitivity (Butcher & Burke, 1994a). The model assumes the formation of a type XI G_{21}:A_{43} base pair and a reversed Hoogsteen base pair between A_{22} and either U_{41} or U_{42}. The importance of retaining N^7 of A_{43} is suggested from results in this study as well as that of previous work (Grasby et al., 1995) and is consistent with the proposed model. Our finding that self-cleavage activities supported by G_{21} mutants were only 8−15-fold lower than supported by the wild type sequence sheds doubt on contribution of more than one hydrogen bond from G_{21}. Furthermore, the fact that G_{21}A resulted in the lowest self-cleavage constant of all base variants in this position is inconsistent with N^3 of G_{21} being involved in a hydrogen bond as assumed by the model, since this position would be retained in the G_{21}A mutant.

A model based on functional group substitutions has been suggested (Schmidt et al., 1996). From our results of this study, the proposed G_{21}:U_{42} wobble or reverse wobble base pairs in this model are unlikely on the basis of the ability of G_{21} mutants to support cleavage rates only one order of magnitude less that the wild type sequence. In addition, the suggested C_{25}:U_{37} interaction was not supported by our results on the basis of the high levels of catalysis supported by each of the U_{37} base variants.

A possible interaction in these proposed models which is not inconsistent with our results is a proposed $A_{22}-U_{41}$ interaction. This was proposed based on the requirement for both of these bases for cleavage−ligation or for cleavage with the substitutions used. However, cleavage assays have found significant activity for U_{41}C (Anderson et al., 1994; Table 1). In order to verify such an interaction, alternate base pair mutations in addition to inactivating and mismatch mutations would need to be done. To date these have not been done for this proposed interaction.

An interaction consistent with previous mutagenesis data (Berzal-Herranz et al., 1993) and supported by this study is a non-canonical A_{26}:G_{36} base pair. This extends helix 4 to 4 bp. Prior to the discovery of this interaction, 17 Watson−Crick base pairs were identified in the hairpin ribozyme (Hampel et al., 1990; Anderson et al., 1994). With the addition of this A_{26}:G_{36} base pair, the structure now has 18 confirmed base−base interactions.

Figure 1 summarizes these results to date in the form of a proposed two-dimensional model. The model is modified from the originally proposed L-shaped configuration (Hampel et al., 1989; Altschuler et al., 1992). While a hinge exists between these two helices (Feldstein & Bruening 1993; Komatsu et al., 1994; Anderson et al., 1994), the exact angle is not known. This model for the hairpin ribozyme has the 18 bp found in the four helices interspersed by the five single-stranded loops. To date, no additional base pairs or interactions in opposing strands of the structure have been identified.

Most studies to date have focused on attempting to find interactions between the bases of loops 2 and 4. However, with the existence of a hinge between helices 2 and 3 allowing the molecule to fold back on itself such that helices 2 and 3 are not co-axial, interactions on an *a priori* basis are just as likely to occur between any combination of loops 1, 2, 4, and 5. Thus future analyses of base−base interactions must include these additional possibilities.

REFERENCES

Altschuler, M., Tritz, R., & Hampel, A. (1992) *Gene 122*, 85−90.

Anderson, P., Monforte, J., Tritz, R., Nesbitt, S., Hearst, J., & Hampel, A. (1994) *Nucleic Acids Res. 22*, 1096−1100.

Berzal-Herranz, A., Joseph, S., & Burke, J. (1992) *Genes Dev. 6*, 129−134.

Berzal-Herranz, A., Joseph, S., Chowrira, B. M., Butcher, S., & Burke, J. (1993) *EMBO J. 12*, 2567−2574.

Butcher, S., & Burke, J. (1994a) *Biochemistry 33*, 992−999.

Butcher, S., & Burke, J. (1994b) *J. Mol. Biol. 244*, 52−63.

Buzayan, J., Gerlach, W., & Bruening, G. (1986) *Nature 323*, 349−352.

Chowrira, B., Pavco, P., & McSwiggen, J. (1994) *J. Biol. Chem. 269*, 25856−25864.

DeYoung, M. B., Siwkowski, A., Lian, Y., & Hampel, A. (1995) *Biochemistry 34*, 15785−15791.

Feldstein, P., & Bruening G. (1993) *Nucleic Acids Res. 21*, 1991−1998.

Gerlach,W., Buzayan, J., Schneider, I., & Bruening, G. (1986) *Virology 151*, 172−185.

Grasby, J., Mersmann, K., Singh, M., & Gait, M. (1995) *Biochemistry 34*, 4068−4076.

Hampel, A., & Tritz, R. (1989) *Biochemistry 28*, 4929−4933.

Hampel, A., Tritz, R., Hicks, M., & Cruz, P. (1990) *Nucleic Acids Res. 18*, 299−304.

Hegg, L., & Fedor, M. (1995) *Biochemistry 34*, 15813−15828.

Herschlag, D. (1995) *J. Biol. Chem. 270*, 20871−20874.

Komatsu,Y., Koizumi, M., Nakamura, H., & Ohtsuka, E. (1994) *J. Am. Chem Soc. 116*, 3692-3696.

Long, D., & Uhlenbeck, O (1993) *FASEB J. 7*, 25−30.

Long, D., & Uhlenbeck, O. (1994) *Proc. Natl. Acad. Sci. U.S.A 91*, 6977−6981.

Milligan, J., Groebe, D., Witherell, G., & Uhlenbeck, O. (1987) *Nucleic Acids Res. 15*, 8783−8798.

SantaLucia, J., Kierzek, R., & Turner, D. (1990) *Biochemistry 29*, 8813−8819.

Schmidt, S., Beigelman, L., Karpeisky, A., Usman, N., Sorensen, U., & Gait, M. (1996) *Nucleic Acids Res. 24*, 573−581.

Welch, P., Hampel, A., Barber, J., Wong-Staal, F., & Yu, M (1996) in *Nucleic Acids and Molecular Biology, Vol. 10: Catalytic RNA* (Eckstein, F., & Lilley, D. M. J., Eds.) pp 315−327, Springer, Berlin.

BI9628735